EUROPEAN TRANSACTIONS ON TELECOMMUNICATIONS
Eur. Trans. Telecomms. (2010)
Published online in Wiley Online Library
(wileyonlinelibrary.com) DOI: 10.1002/ett.1434

Optimal soft frequency reuse and dynamic sub-carrier assignments in cellular OFDMA networks†

Mathias Bohge[1]*, James Gross[2] and Adam Wolisz[1,3]

[1]*Technische Universität Berlin, TKN Group, Einsteinufer 25, 10587 Berlin, Germany*
[2]*RWTH Aachen University, UMIC Research Centre, Mies-van-der-Rohe-Str. 15, 52074 Aachen, Germany*
[3]*University of California, Berkeley, BWRC, 2108 Allston Way, Suite 200, Berkeley, CA 94704-1302, USA*

SUMMARY

Soft frequency reuse (SFR) is a common technique for co-channel interference (CCI) mitigation in cellular OFDMA networks. The performance of such networks significantly depends on the configuration of the power profiles that implement the soft frequency reuse patterns. In this paper, we investigate the performance of static soft frequency reuse by comparing it against the optimal case, in which a central entity optimally distributes power among the users of the network. It is shown that there is a significant performance gap between both approaches, which needs to be filled by adaptive SFR mechanisms. Moreover, we show that the achievable gain of static SFR is small in a system that is able to optimally decide on terminal/sub-carrier assignments. Copyright © 2010 John Wiley & Sons, Ltd.

1. INTRODUCTION

Orthogonal frequency division multiplexing (OFDM) today is the dominant physical layer transmission scheme in broadband wireless systems. Over the last decade, this transmission scheme has been combined with multiple access into a scheme known as orthogonal frequency division multiple access (OFDMA). In OFDMA disjoint sets of sub-carriers are assigned to different terminals for transmission over a certain time period. As this can be combined with channel-state dependent resource allocation, resulting system performance is high. Therefore, OFDMA is a promising technique for use in various systems and scenarios. While the application of OFDMA in single-cell settings is well understood (see References [1–3]), a key open issue with the application of orthogonal frequency division multiple access in mobile cellular systems is the control of co-channel interference. Especially terminals located at the cell border largely suffer from the power radiated by the base station of neighbouring cells in their communication band.

During the last couple of years, soft frequency reuse (SFR) [4] has been established as a standard technique to control CCI in cellular OFDMA systems. With SFR, a reuse factor of one is applied between neighbouring cells, but for the transmission on each sub-carrier the base stations are restricted to a certain power bound. The amount of power that is allowed to be radiated on a specific part of the spectrum is defined by cell-specific *power profiles* (*cf.* Figures 2 and 5). Initially, the power profiles have been assumed to be of static nature and hence do not adapt to the current traffic situation [5]. Lately, in References [6–8], the possibility is explored to dynamically adapt power profiles as part of self-organisation in a network (SON). These dynamic approaches show a performance gain compared to the static approach. They, however, do not answer the question on how much gain can be expected, if the power profiles could be *optimally* configured to mitigate CCI.

* Correspondence to: Mathias Bohge, Technische Universität Berlin, TKN Group, Einsteinufer 25, 10587 Berlin, Germany. E-mail: bohge@tkn.tu-berlin.de
† A previous version of this paper was presented in the 15th European Wireless Conference (EW 2009), Aalborg, Denmark.

Received 1 December 2009
Accepted 20 April 2010

In this paper we give an answer to this question. Our central contribution is the formulation of an according global knowledge exploiting nonlinear optimisation problem. Despite the high problem complexity, several according problem instances are solved in a basic reference scenario. Moreover, we answer the related question concerning the benefit of using static power profiles in a system with an optimal dynamic terminal/sub-carrier assignment strategy.

The reminder of this paper is organised as follows. In the following section, our system model is introduced. In the section thereafter, the potential of adaptive soft frequency reuse to mitigate CCI is explored by comparing the performance results of a globally optimal working system to those of a system applying either no CCI mitigation mechanism, a static soft frequency reuse approach, or a legacy hard frequency reuse (HFR) scheme in a basic scenario. The benefit of using static power profiles in a system with an optimal dynamic terminal/sub-carrier assignment strategy is studied in more detail in a more realistic scenario in the subsequent section. Finally, we conclude our work and identify topics for further study in the final section.

2. SYSTEM MODEL

Throughout this paper, the downlink (DL) of an OFDMA based cellular system with site-to-site distance d_{s2s} is considered. Within each cell, a base station coordinates all data transmissions. J terminals are uniformly distributed over the considered area, each moving with speed v according to the Manhattan grid mobility model.

2.1. Wireless channel model

In general, the impact of the wireless channel on the transmitted data is expressed as one signal-to-noise and interference ratio value $\gamma^{(t)}_{c,j,s}$ per cell c, terminal j, sub-carrier s and time instance t:

$$\gamma^{(t)}_{c,j,s} = \frac{h^{(t)}_{c,j,s}\, p^{(t)}_{c,s}}{\sum\limits_{c_i \neq c} h^{(t)}_{c_i,j,s}\, p^{(t)}_{c_i,s} + \sigma^2_{\eta,s}} \tag{1}$$

Here, $h^{(t)}_{c,j,s}$ is the gain experienced by terminal j on sub-carrier s at time t versus the base station of cell c, $p^{(t)}_{c,s}$ is the power radiated by the base station of cell c on sub-carrier s at time t, and $\sigma^2_{\eta,s}$ is the noise power present on sub-carrier s. Gain $h^{(t)}_{c,j,s}$ is commonly modelled by the composition of three factors: *path loss* h_{PL}, *shadowing* h_{SH}, and *fading* h_{FA}. To model path loss, we use the following empirical approach suggested for LTE macro-cell system simulations by the 3GPP in Reference [9] (Table A.2.1.1-3):

$$h_{PL}[\mathrm{dB}] = 128.1 + 37.6 \log_{10}(d) \tag{2}$$

where d is measured in kilometers. A penetration loss value of 20 dB is added in accordance with simulation case 1 of Table A.2.1.1-1 of Reference [9]. Also in accordance with Reference [9] (Table A.2.1.1-3), shadowing is modelled as a lognormal random variable with a standard deviation σ_{sh} of 8 dB. Fading is modelled as Rayleigh fading according to 3GPP's spatial channel model 'Urban Macro' with a median root-mean square delay of 0.65 μs. In the case of stationary terminals, we assume fading to be present due to objects moving within the system area at a speed of $v = 3\,\mathrm{m/s}$.

2.2. Link level performance model

The task of the link level performance model in simulations is to translate the channel quality experienced by a receiver into receiver performance in terms of, for example, capacity, throughput or error values. In general, function F denotes the mapping between channel quality (expressed by the SNIR) and the achievable capacity or throughput. A popular link level performance model is the Shannon capacity

$$\vartheta_{\mathrm{shannon}}[\mathrm{bps}] = B \log_2(1 + \gamma) \tag{3}$$

It represents the an upper limit on the error-free throughput than can be achieved over an AWGN channel for a given SNR [10]. We assume that this applies also in scenarios where interference is present and use the Shannon capacity in the basic investigations of section 'Basic Multi-Cell OFDMA Investigations'.

For the more detailed investigations of section 'Extended SCA and SFR Examinations', we use a more realistic model suggested by the 3rd Generation Partnership Project (3GPP) for LTE link level simulations [11]. It assumes that the throughput of a modem with adaptive coding and modulation can be approximated by an attenuated and truncated form of the Shannon bound. The following equations approximate the throughput ϑ in bits-per-second (bps) over a channel with a given SNIR γ, when using link adaptation:

$$\vartheta_{\mathrm{tc}}[\mathrm{bps}] = \begin{cases} 0 & \text{for } \gamma < \gamma_{\min} \\ \alpha_{\mathrm{tc}} B \log_2(1+\gamma) & \text{for } \gamma_{\min} < \gamma < \gamma_{\max} \\ \beta_{\mathrm{tc}} B & \text{for } \gamma > \gamma_{\max} \end{cases} \tag{4}$$

DOI: 10.1002/ett

Table 1. Parameters describing baseline link level downlink performance for LTE simulations.

Parameter	Symbol	Value	Notes
Attenuation factor	α_{tc}	0.6	Represents implementation losses
Maximum throughput in bps/Hz	β_{tc}	4.4	Based on 64QAM, code rate 4/5
Minimum SNIR in dB	$\gamma_{\min}$	-10	Based on QPSK, code rate 1/8

where B is the channel bandwidth, α_{tc} is the attenuation factor, representing implementation losses, β_{tc} maximum throughput of the ACM codeset in bps/Hz, and $\gamma_{\min}$ and $\gamma_{\max}$ in dB are the minimum SNIR of the codeset, and the SNIR at which maximum throughput is reached, respectively. The parameterization of α_{tc}, β_{tc} and $\gamma_{\min}$ is chosen as suggested in [11] and is summarized in Table 1.

2.3. Physical layer model

The system under consideration uses orthogonal frequency division multiplexing as transmission scheme for downlink data transmission. It features a total bandwidth of B at center frequency f_{c}. The given bandwidth is split into S sub-carriers, each featuring a bandwidth (also referred to as sub-carrier frequency spacing) of $\Delta f = B/S$. The maximum transmit power per cell $p_{\max}$ is split among the sub-carriers. Time is slotted into transmission time interval (TTIs) of duration T_{TTI}, where T_{TTI} is assumed to be smaller than the coherence time of the wireless channel (i.e. in the order of milliseconds). Hence, the atomic resource unit has a size of one OFDM symbol length T_{S} in the time domain and one sub-carrier bandwidth Δf in the frequency domain, and is referred to as resource element (RE) (see Figure 1). Prior to the transmission of the time domain OFDM symbol, a cyclic prefix of length T_{g} is added as guard interval.

2.4. Medium access layer model

Data multiplexing in the downlink is based on orthogonal frequency division multiple access, where the smallest *allocatable* resource unit is a *resource block* (*RB*) n (*cf.* Figure 1). An RB consists of a number of adjacent REs in the frequency domain (sub-carriers) N_{subs} and spans all REs available for user data transmission of a TTI [9].

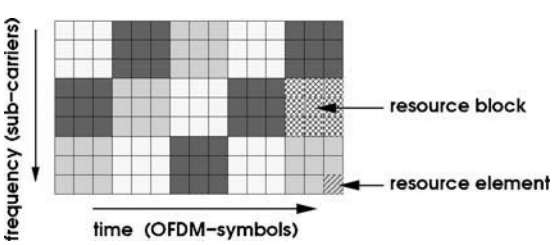

Figure 1. Example resource blocks (RBs) consisting of 9REs.

The RB bandwidth (number of REs in the frequency domain) is chosen, such that channel quality differences among the sub-carriers belonging to a single resource block are negligible (i.e. the RB is assumed to experience mostly flat fading). If N_{subs} is the number of adjacent sub-carriers (REs in the frequency domain) belonging to a single resource block n, the number of available RBs to transmit data per TTI is $N = S/N_{\text{subs}}$.

2.4.1. Scheduling decisions. At the beginning of each TTI, a base station scheduler assigns RBs to the terminals in each cell c. The distribution of the RBs among the terminals has a significant impact on the system performance. A rather simple scheduler assigns the resource blocks *statically* (i.e. following a certain recurring pattern), as for example, the round robin (RR) scheduler. Statically assigning the resources yields the advantage that the resource allocations do not need to be signaled more than once. More sophisticated schedulers assign the resources following an optimisation strategy [3]. In this paper, optimal scheduling strategies are explored (as described in the next section), whereas the simple RR scheduler serves as a benchmark. It is also the scheduler's task to distribute the maximum available transmission power $p_{\max}$ among the RBs. Within each RB n all sub-carriers s obtain the same power share.

3. BASIC MULTI-CELL OFDMA INVESTIGATIONS

The investigations of this section aim at an comparison between the performance of systems employing standard hard frequency reuse and soft frequency reuse CCI mitigation techniques and the performance of a globally optimal dynamic power allocation and sub-carrier assignment based system.

3.1. Global optimisation

A major assumption in the global optimisation case is that the optimal resource scheduling decision at time t is made at

DOI: 10.1002/ett

a single point (referred to as *central entity*), at which unlimited computational power and ideal system-wide knowledge is available. Particularly, the central entity is in charge of determining the optimal real-valued power levels $y_{c,s}^{(t)}$ for each sub-carrier in each cell c out of the set of active cells C, as well as for finding the optimal binary terminal/sub carrier assignments $x_{c,j,s}^{(t)}$ at time t, where

$$x_{c,j,s}^{(t)} = \begin{cases} 1, & \text{if in } c \text{ sub-carrier } s \text{ is assigned to } j \text{ at } t \\ 0, & \text{if in } c \text{ sub-carrier } s \text{ is not assigned to } j \text{ at } t. \end{cases}$$

Integrating the power and sub-carrier assignment optimisation variables into a single optimisation problem that maximises the system throughput yields the nonlinear global OFDMA resource allocation formulation:

$$\max_{\mathbf{X}^{(t)},\mathbf{Y}^{(t)}} \sum_{\check{c}=1}^{C}\sum_{j=1}^{J_c}\sum_{s=1}^{S} x_{\check{c},j,s}^{(t)} F\left(\frac{h_{\check{c},j,s}^{(t)} y_{\check{c},s}^{(t)}}{\sigma_\eta^2 + \sum\limits_{\forall c \neq \check{c}} h_{c,j,s}^{(t)} y_{c,s}^{(t)}}\right) \quad (5a)$$

$$\text{s.t} \sum_{s=1}^{S} y_{c,s}^{(t)} \leqslant p_{\max} \qquad \forall\, c \quad (5b)$$

$$\sum_{j=1}^{J} x_{c,j,s}^{(t)} \leqslant 1 \qquad \forall\, c, s \quad (5c)$$

where $\mathbf{X}^{(t)}$ is the $C \times J \times S$ matrix of terminal/sub-carrier assignments and $\mathbf{Y}^{(t)}$ is the $C \times S$ matrix of power assignment variables at time t, J_c is the number of terminals in cell $\check{c}$, and $F(\ldots)$ is the link level performance function that determines the throughput depending on the instantaneous SNIR. Note that there is a twofold nonlinearity property in optimisation goal (5a): firstly, optimisation variable $y_{c,s}^{(t)}$ is present in the nominator, as well as in the denominator of SNIR term, reflecting that a better power distribution in one cell might lead to a worse situation in another cell. Secondly, there is a nonlinearity due to the multiplication of the terminal/sub-carrier optimisation variable $x_{c,j,s}^{(t)}$ and the power allocation optimisation variable $y_{c,s}^{(t)}$ dependent $F()$ term. Due to these nonlinearities and additional integer constraints *global constrained max sum rate* problem (5) is very hard to solve. Furthermore, it requires all channel attenuations to be known at the central entity for all sub-carriers, terminals and base stations. Hence, this scheme serves pure comparison purposes representing an upper bound.

In order to account for intra-cell fairness, *required throughput per terminal* constraint (5d) is added to form the complete *global constrained max sum rate problem*:

$$\sum_{s=1}^{S} x_{j,s}^{(t)} F\left(\frac{h_{\check{c},j,s}^{(t)} y_{\check{c},s}^{(t)}}{\sigma_\eta^2 + \sum\limits_{\forall c \neq \check{c}} h_{c,j,s}^{(t)} y_{c,s}^{(t)}}\right) \leqslant \vartheta_{\text{req},j} \qquad \forall\, cj \quad (5d)$$

Here, it is assumed that for each terminal j there is a required throughput $\vartheta_{\text{req},j}$, and that any throughput beyond $\vartheta_{\text{req},}$ is useless. In other words, the overall optimisation goal is to maximise the system throughput while assuring that none of the users gets more than its required rate. This approach corresponds to a simple piecewise linear utility function.

3.2. Local optimisation employing standard CCI mitigation techniques

In the case of local optimisation, the base station schedulers of each cell make individual scheduling decisions per cell, i.e. no central entity is involved. Each scheduler relies on local information only. All sub-carrier assignment decisions in cell $\check{c}$ are made by solving the according instance of the *local constrained max sum rate* problem:

$$\max_{\mathbf{X}^{(t)}} \sum_{j=1}^{J_c}\sum_{s=1}^{S} x_{\check{c},j,s}^{(t)} F\left(\gamma_{\check{c},j,s}^{(t)}\right) \quad (6a)$$

$$\text{s.t} \sum_{j=1}^{J_c} x_{\check{c},j,s}^{(t)} \leqslant 1 \qquad \forall\, s, \quad (6b)$$

$$\sum_{s} x_{\check{c},j,s}^{(t)} F\left(\gamma_{\check{c},j,s}^{(t)}\right) \leqslant \vartheta_{\text{req},j} \quad \forall\, j \in J_c \quad (6c)$$

Since merely local information is available at each scheduler, there is no opportunity to optimise the power allocation per sub-carrier in order to mitigate CCI, as it is done in the global optimisation approach. Instead, standard HFR or SFR is used to suppress CCI. Recall that when applying HFR or SFR power profiles can be used to prescribes the fraction of the maximum transmit power that the base station may use depending on the part of the spectrum. In the following, the power profile of cell $\check{c}$ is denoted by $\pi_{\check{c},s} \in [0, 1]$. It denotes the fraction of the total available output power $p_{\max}$. On sub-carrier s, cell $\check{c}$ thus transmits with a power of $p_{\max}\pi_{\check{c},s}$. Considering power profiles, the SNIR experienced by terminal j on sub-carrier s in cell $\check{c}$

DOI: 10.1002/ett

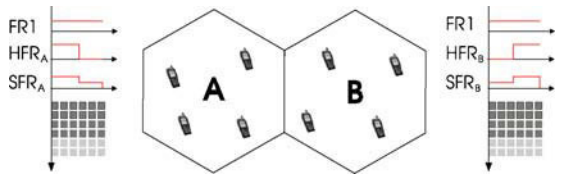

Figure 2. Reference scenario for the basic investigations.

can be written as

$$\gamma_{\check{c},j,s}^{(t)} = \frac{\pi_{\check{c},s} p_{\max} h_{\check{c},j,s}^{(t)}}{\sum\limits_{\substack{c=1 \\ c\neq\check{c}}}^{C} \pi_{c,s} p_{\max} h_{c,j,s}^{(t)} + \sigma_{\eta,s}^2} \tag{7}$$

The above denominator sums up the CCI from concurrently sending base stations $c \neq \check{c}$ and the noise power $\sigma_{\eta,s}^2$.

3.3. Basic multi-cell reference scenario

The basic reference scenario is shown in Figure 2. It adopts the system model described in section 'System Model'. Shannon capacity is assumed as link level performance model in order to achieve the theoretical optimum and refrain from clipping effects that might appear when using the truncated Shannon link level performance model (*cf.* subsection 'Link Level Performance Model').

3.3.1. Parameterisation. The simulation parameterisation largely follows the parameters for the LTE simulation case 1 as presented in Tables A.2.1.1-1 and A.2.1.1-2 of Reference [9] with an inter-site distance of 500 m and users dropped uniformly in each hexagonal cell. In this basic reference scenario, however, two hexagonal cells are considered only. The reason for this is that for significantly larger scenarios, the *global constrained max sum rate* problem (5) is not solvable within reasonable time bounds using regular hard- and software equipment. Notwithstanding standard [9], which defines 25 resource blocks for a 5 MHz system, the basic reference model features 24 resource blocks with a resource block spacing of 200 kHz. The reason for that is that 24 is divisible by two, which allows fair resource sharing among the two cells in the HFR and the SFR scenario. Each resource block consists of 12 adjacent sub-carriers. Eight terminals, four in each cell, are uniformly distributed over the cell area. In the SFR case, the power profiles are configured such that the high power level is ten times the low power level. Accordingly, each base station radiates $1/11 \cdot p_{\max}$ on one half of spectrum and with $10/11 \cdot p_{\max}$ on the other half.

3.3.2. Methodology. The wireless channel as well as the terminal mobility are simulated according to the system model presented in section 'System Model'. At the beginning of each TTI a snapshot of the current CSI values per terminal and base station is taken. These snapshot values are used to create optimisation problem instances following the optimisation models presented in section 'Basic Multi-Cell OFDMA Investigations'. In the case of global optimisation, one global scheduling problem instance is created *per TTI* and piped into LINDO's LINGO nonlinear optimisation problem solver [12]. If local optimisation is selected, one local scheduling problem instance *per cell and TTI* (i.e. a total number of C problem instances) needs to be solved per TTI. To solve the local problem instances, they are piped into ILOG's CPLEX linear problem solver [13].

After solving the individual instances, the solving software pipes back the optimal scheduling decisions into the simulator software that uses it for further processing and throughput calculations. The simulator is based on the free timed discrete event simulation library OMNeT++ [14]. Different required rate per terminal threshold $\vartheta_{\text{req},j}$ scenarios have been explored ranging from 2 to 5 Mbps. In each scenario 100 different user distributions have been simulated, resulting in a high level of confidence (as can be seen from the confidence intervals in the result figures).

3.4. Results

For each scenario, the mean cell throughput, the mean throughput of the weakest (cell-edge) terminal of the system, as well as the individual per terminal throughputs are presented. For the first two, error bars display confidence intervals with a confidence level of 99 %.

The first result that catches the eye when examining the weakest terminal throughput performance comparison in Figure 3a is fact that the global optimal weakest user throughput grows linearly with the required rate per terminal value. For a required throughput per terminal of $\vartheta_{\text{req},} =$ 5 Mbps the weakest terminal's throughput is 5Mbps, i.e. that all terminals achieve the required throughput. This fact is also reflected in Figure 4d that shows the individual mean terminal throughput in the case of global optimisation. The very narrow 99% confidence intervals in Figure 3a indicate that this is true for all simulation runs. Accordingly, the system throughput performance achieves its maximum per cell throughput of 20 Mbps.

Altogether, the application of global optimisation in the basic reference scenario achieves significant cell-edge terminal throughput performance gains of up to 100% and

DOI: 10.1002/ett

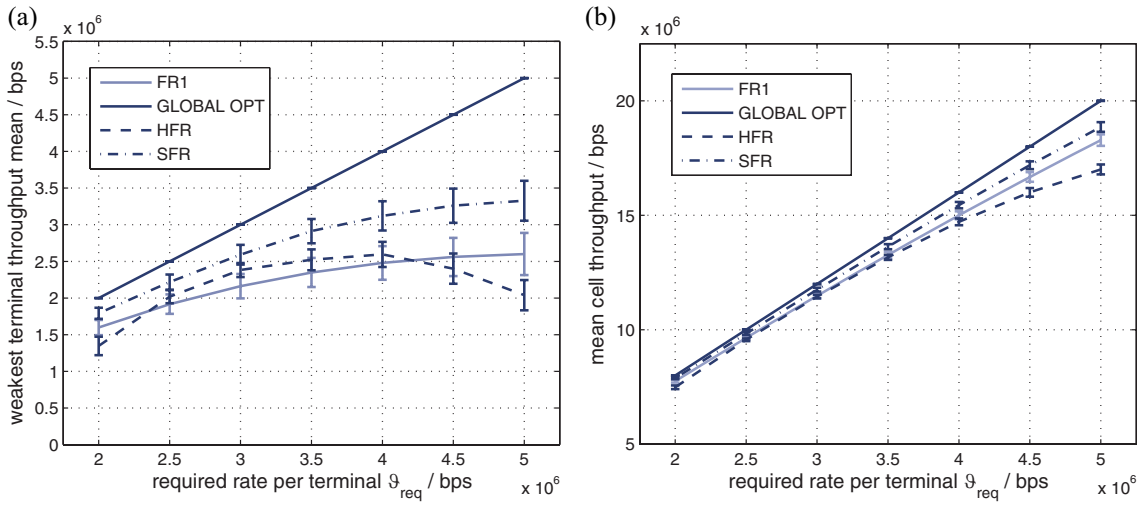

Figure 3. Basic reference model throughput performance results: (a) mean throughput (bps) of weakest terminal and (b) mean cell throughput (bps).

system throughput gains of more than 10% compared to the frequency reuse 1 scenario, in which no CCI mitigation techniques are applied. Obviously, the application of sub-optimal CCI mitigation mechanisms delivers less strong results. Comparing HFR to FR1, the graphs show that the application of HFR hardly improves the cell edge terminal performance, even though up to a required rate of 4 Mbps HFR performs slightly better. The small advantage are due to the fact that there is zero interference from the neighbour cell, and, thus, the channel states of the cell edge terminals are generally better than in the frequency reuse 1 case. Due to the limited resources in the hard frequency reuse case, however, the weakest terminals cannot take advantage of the increasing required rate above that 4 Mbps threshold. This is mainly because the cell edge terminals hardly get any resources at all, if the terminals at the center are allowed to consume resources for such high rates. Accordingly, their mean throughput decreases with the increasing required rate after that turning point.

Greater performance gains can be achieved, if SFR is applied. Figure 3a shows a performance gain in cell edge terminal throughput over FR1 of up to 30 %. This is an immense gain, considering the fact that the gain solely stems from masking the resource block power levels. Note that the weakest terminal's throughput gain is present in all chosen required rate per terminal cases, and that it constantly grows with an increasing required rate. In contrast to HFR, even the overall system performance gains slightly, if SFR is applied.

This result underlines the assumption that dynamic power and sub-carrier assignment techniques bear a high potential to mitigate CCI in cellular OFDMA networks. Note, however, that the gains have been achieved under idealistic conditions.

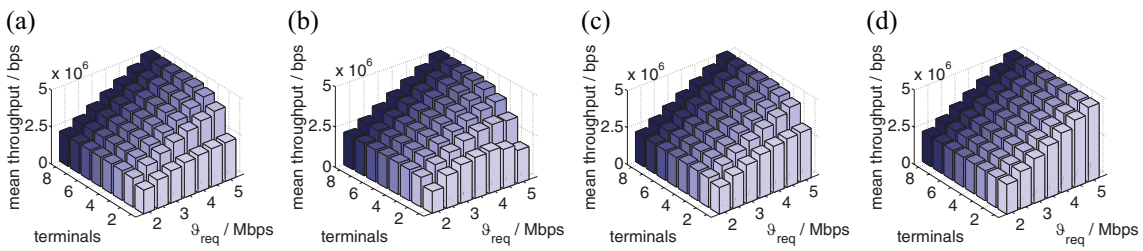

Figure 4. Individual mean terminal throughput results: (a) frequency reuse 1, (b) hard frequency reuse, (c) soft frequency reuse and (d) global optimisation.

DOI: 10.1002/ett

4. EXTENDED SCA AND SFR EXAMINATIONS

In this section, the application of dynamic sub-carrier assignment and soft frequency reuse is studied under more realistic conditions. Particularly, the network size and the CSI availability are modelled closer to reality.

Increasing the hexagonal network size yields an increased impact of CCI in both, the FR1 case (where all neighbouring cells use the same frequency band), as well as in the SFR case (where power profiles are reused in different cells). In terms of CSI availability, in the previous section CSI was assumed to be available at any point in time and the scheduler was assumed to be able to adapt to it immediately. Obviously, in real systems these values are not instantly available. The scheduler, thus, has to work with delayed channel measurements. Note that the advantage of a highly accurate adaptation to the channel state in the optimal case can turn into a disadvantage in reality. Therefore, in this section the impact of CSI processing delay ΔT_{csi} on the performance of the dynamic sub-carrier allocation and power profiling combination in multi-cell scenarios is studied. Different time spans between the measurement of channel state information and its actual usage for channel adaptation are considered. We assume the scheduler to use the most recent SNIR value available from the terminals to estimate the current capacity per terminal/sub-carrier pair.

4.1. Extended multi-cell reference scenario

The extended reference scenario is shown in Figure 5a. It adopts the system model described in section 'System Model'. The truncated Shannon link level performance model (*cf.* section 'Extended SCA and SFR Examinations') is used.

4.1.1. Parameterisation. The extended reference system and channel model parameterisation largely follows the parameters for the LTE simulation case 1, as presented in Tables A.2.1.1-1 and A.2.1.1-2 of Reference [5] with an inter-site distance of 500 m and terminals dropped uniformly over the system area. Additional parameters are summarised in Table 2.

Table 2. Extended multi cell reference model parameters.

Parameter	Symbol	
Number of cells	C	7
Number of terminals	J	70
Terminal speed	v	$\{0; 10\}$ m/s
Req. throughput per terminal	$\vartheta_{\text{req},j}$	1 Mbps
RB freq. spacing	Δf_n	200 kHz
Number of RBs	N	25
Sub-carriers per RB	N_{subs}	12
CSI processing delay	ΔT_{csi}	$\{0 \ldots 5\}$ TTIs

4.1.2. Power profiles. In contrast to the basic reference scenario, in this section SFR3 profiling is assumed, i.e. each power profile features three different power levels: high, middle and low (as shown in Figure 5). Each cell uses one third of the spectrum with each power level. Two different standard SFR power profile types are considered:

- $\text{SFR}_{[1;0.5;0.25]}$: the low power level equals one forth and the medium equals half of the high power level.
- $\text{SFR}_{[1;0.1;0.01]}$: the low power level equals one hundredth and the medium level equals one tenth of the high power level.

In order to stick to a consistent notation, we also assume a power profile for the FR1 case, in which the power is uniformly distributed over the sub-carriers: the uniform power profile, where $\pi_{c,n} = p_{\max}/N$ for all n and c (where N is the number of available resource blocks).

4.1.3. Methodology. The OFDMA system-level simulation and the integration of the linear optimisation problem solver has been done as described for the basic reference scenario in section 'Basic Multi-Cell OFDMA Investigations'. Initially, the performance of plain dynamic sub-carrier assignment (i.e. in the FR1 case) is compared to a benchmark system that statically assigns the sub-carriers among the terminals in a round robin fashion. The goal is to determine its performance subject to large CCI and an increasing CSI processing delay. Then, SFR is applied on top of the dynamic SCA techniques.

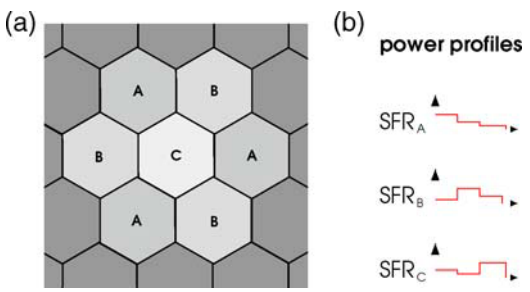

Figure 5. Extended reference scenario with SFR power profiling: (a) hexagonal multi-cell layout and (b) cell configuration .

DOI: 10.1002/ett

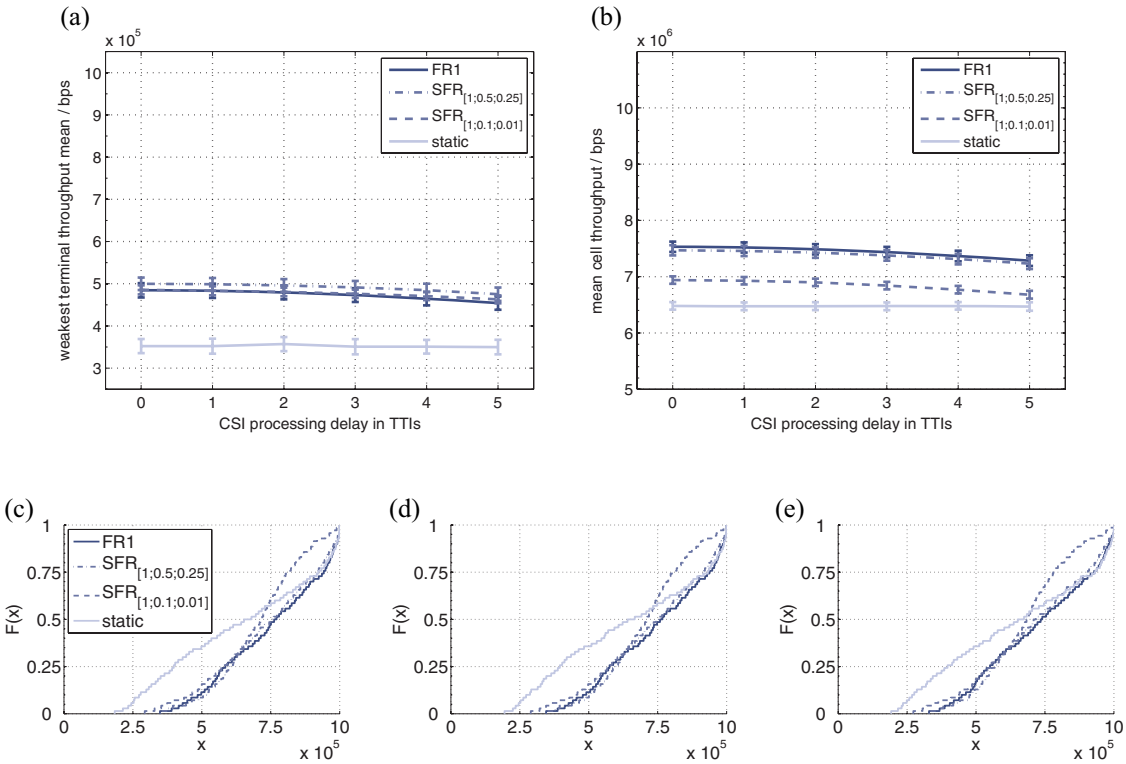

Figure 6. The gain of applying SFR on top of optimal SCA, *stationary terminals*: (a) mean throughput (bps) of weakest terminal, (b) mean cell throughput (bps), (c) per terminal throughput cdf, 0 TTIs, (d) per terminal throughput cdf, 2 TTIs and (e) per terminal throughput cdf, 5 TTIs.

4.2. Results

We start discussing the results by considering a scenario with stationary terminals.[‡] In Figure 6 the average throughput of the weakest terminal as well as the mean cell throughput are shown for different CSI processing delays. Let us first focus on the average throughput of the weakest terminal. We observe a significant throughput gain stemming from dynamic sub-carrier assignments (in comparison to the round robin scheduler). Due to the low time variability of the channel, the impact of the CSI processing delay is rather low. While the RR scheduler is not effected by the processing delay, the dynamic schemes suffer slightly (at most 10% throughput loss). Still, at the highest processing delay the dynamic schemes outperform the RR scheme by at least 30%. Among the dynamic schemes, for the weakest terminal throughput the applied power profile is less important. This is quite surprising in comparison to the results of section 'Basic Multi-Cell OFDMA Investigations' as especially the FR1 scheme should perform worse than the SFR schemes. Next, focus on the average cell throughput also presented in Figure 6. Regarding this total throughput of the cell, the advantage of dynamic (optimal) scheduling is still present (compared to the RR scheme), however, the application of power profiles starts to become important. In the case of SFR with a profile of $[1; 0.1; 0.01]$ the mean cell throughput is significantly lower than for the other two dynamic schemes. This is due to too much power allocated in the first bandwidth partition and too less power assigned in the other partitions. Altogether, this leads to a performance loss of roughly 10% compared to the other SFR and the FR1. Still, the loss due to delayed CSI information is rather low and all dynamic system approaches outperform the RR scheme. In addition to the average throughput plots, we also provide in Figure 6 graphs showing the CDFs of the average throughput of the terminals within the considered cells. Here, the main statements from above are confirmed. Notice in particular, that dynamic subcarrier assignments do improve not only the situation of the absolute worst terminal

[‡] Note that we still assume some objects within the propagation environment to be mobile causing fading effects in frequency and time (see section 'System Model').

DOI: 10.1002/ett

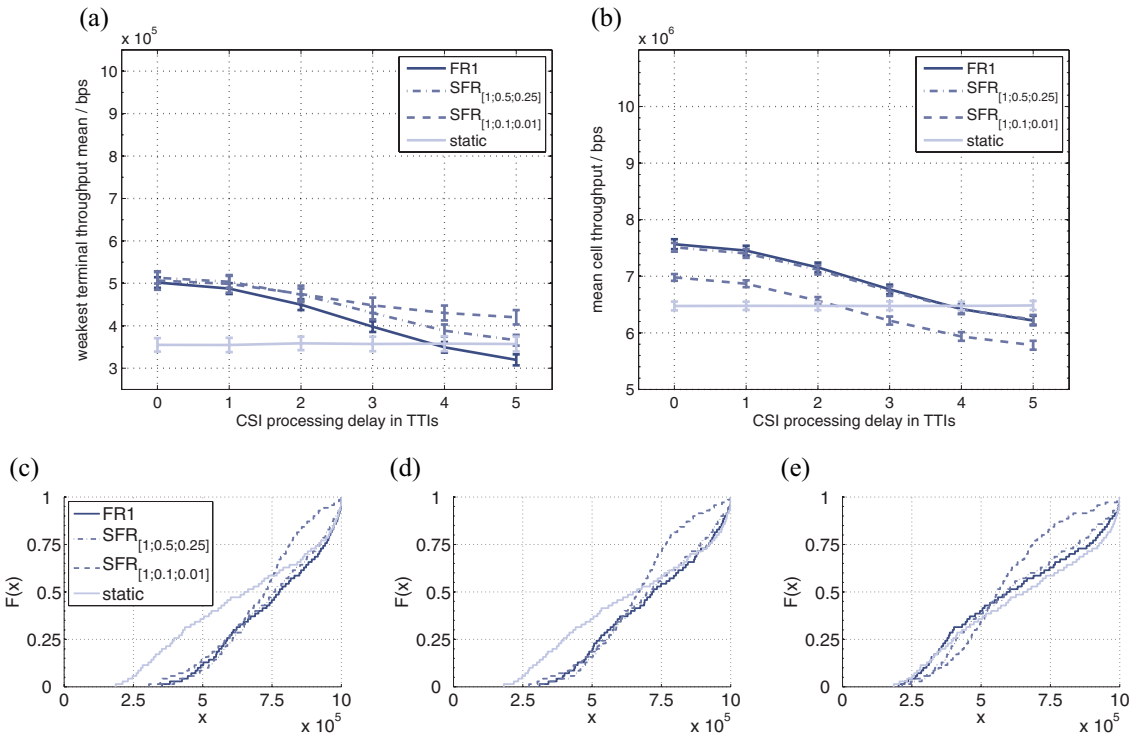

Figure 7. The gain of applying SFR on top of optimal SCA, *moving terminals*, speed $v = 10\frac{m}{s}$: (a) mean throughput (bps) of weakest terminal, (b) mean cell throughput (bps), (c) per terminal throughput cdf, 0 TTIs, (d) per terminal throughput cdf, 2 TTIs and (e) per terminal throughput cdf, 5 TTIs.

but of about 75% of the terminals present in the cell. Especially for the lowest quartile, the average throughput gain is quite significant for all considered power profiles (about 70% in case of no processing delay, which reduces to 50% in case of the longest processing delay considered). In these CDF plots we also observe the impact of choosing a strict power profile, as is the case with SFR $[1; 0.1; 0.01]$. Compared to the other SFR scheme, especially the throughput of the strongest terminals is reduced due to the lower transmit power setting (at no significant throughput advantage for the terminals in the lowest quartile).

This overall picture partially changes if the channel becomes more time variable. In Figure 7 we show the corresponding results for terminals moving with a speed of $v = 10\,\mathrm{m/s}$. In general we observe that for the throughput of the weakest terminal as well as for the total cell the processing delay becomes important. For the largest considered processing delay, the performance of all dynamic schemes with optimal sub-carrier assignments drops below the performance of the round robin scheduler. This is simply due to outdated channel information which can not provide the resource allocation algorithm a valid decision base any more. In fact, sub-carrier assignment could also be done random. However, for the weakest terminal there is a floor that the SFR scheme with power profile $[1; 0.1; 0.01]$ reaches. This is not due to dynamic sub-carrier assignments, instead it results from the strong suppression of interference at the cell border which gives terminals positioned at the cell edge a significantly better SNIR than in all other cases. However, as can be observed from the results regarding the overall cell throughput, this advantage at the cell edges is paid for by an overall lower total cell throughput. This is also reflected by the results regarding the CDFs of the average terminal throughput of all terminals in all cells, shown also in Figure 7. Here, the performance advantage of the dynamic schemes vanishes as the processing delay increases (in fact, it vanishes for all terminals in the cell). This is not true for the SFR scheme with a power profile setting of $[1; 0.1; 0.01]$, which can achieve some gain for cell edge terminals but at the cost of reducing the performance for terminals in the cell centers. Notice that this performance difference solely stems from the used power profile and not from the dynamic sub-carrier assignments.

Finally, for LTE systems it is commonly assumed that CSI will be delayed by at most 2 TTIs. Taking this into account, it can be observed from the results that dynamic sub-carrier

DOI: 10.1002/ett

assignments provide a much better performance than static RR assignments. Furthermore, there is no clear advantage of SFR compared to FR1 which is in contrast to our findings given im the result of the section 'Basic Multi-Cell OFDMA Investigations'. However, take into consideration that despite the mobility of terminals we have only taken static power profiles into account in case of SFR, leading to less efficient resource distributions throughout all considered cells from time to time. We suspect the optimal system performance to be much higher in this case due to mobility effects.

5. CONCLUSIONS

We have shown that optimally distributing power and subcarriers among the users of a cellular OFDMA network significantly improves the cell edge-user, as well as the overall system performance. Conventional static soft frequency reuse approaches do not exploit this potential, even though they show an advantage over legacy hard frequency reuse and uncontrolled frequency reuse 1 systems. Furthermore, the benefit of applying static SFR in a system with an optimal dynamic terminal/sub-carrier assignment strategy is rather small, which is due to the fact that already solely assigning the sub-carriers dynamically exhibits a high potential to combat co-channel interference in according systems, even if the assignment decisions are based on significantly delayed channel state information.

The development of an SFR power profile adaptation mechanism that approaches the global optimum at low computational costs remains as future work issue.

REFERENCES

1. Wong C, Cheng R, Letaief K, Murch R. Multiuser OFDM with adaptive subcarrier, bit and power allocation. *IEEE Journal on Selected Areas of Communications* 1999; **17**(10): 1747–1758.
2. Rhee W, Cioffi J. Increase in capacity of multiuser OFDM system using dynamic subchannel allocation. In *Proceedings of the IEEE Vehicular Technology Conference (VTC Spring '00)*, vol. 2, May 2000; 1085–1089.
3. Bohge M, Gross J, Meyer M, Wolisz A. Dynamic resource allocation in ofdm systems: an overview of cross-layer optimization principles and techniques. *IEEE Network Magazine, Special Issue: 'Evolution Toward 4G Wireless Networking'* 2007; **21**(1): 53–59.
4. 3GPP, Huawei. *Soft Frequency Reuse Scheme for UTRAN LTE, R1-050507*, May 2005.
5. 3GPP, Huawei. *Further Analysis of Soft Frequency Reuse Scheme, R1-050841*, September 2005.
6. Doppler K, He X, Witjing C, Sorri A. Adaptive soft reuse for relay enhanced cells. In *Proceedings of the IEEE Vehicular Technology Conference (VTC Spring '07)*, April 2007; 758–762.
7. Hernandez A, Guio I, Valdovinos A. Interference management through resource allocation in multi-cell OFDMA networks. In *Proceedings of the IEEE Vehicular Technology Conference (VTC Spring '09)*, April 2009.
8. Stolyar A, Viswanathan H. Self-organizing dynamic fractional frequency reuse for best-effort traffic through distributed inter-cell coordination. In *Proceedings of the 28th IEEE Conference on Computer Communications (Infocom '09)*, April 2009.
9. 3GPP, Technical Specification Group Radio Access Network. *Physical Layer Aspects for Evolved UTRA (Release 7), TR-25.814, Version 1.0.3*, October 2006.
10. Shannon CE. A mathematical theory of communication. *Bell System Technical Journal* 1948; **27**:379-423, 623–656.
11. 3GPP, Technical Specification Group Radio Access Network. *Universal Terrestrial Radio Access (e-utra); Radio Frequency (rf) System Scenarios, TS-36.942, Version 8.1.0*, 2008.
12. LINDO Systems Inc. *LINGO 10—User's Guide*. Chicago: Illinois, 2008.
13. S ILOG. *ILOG CPLEX 10.0—User's Manual*, January 2006.
14. A Varga. *OMNeT++ User Manual 3.2*, March 2005.

DOI: 10.1002/ett